Water-passivated ZnMgO nanoparticles for blue quantum dot light-emitting diodes

Yue Guo,[a] Bochen Liu,[a] Zhao Chen,*[a] Weidong Song,*[a] Naifan Tian,[a] Wenhai Wu,[a] Xiaokun Fan,[a] Yunfeng Zhan,[a] Fanyuan Meng[a], Qingguang Zeng[a] and Wai-Yeung Wong*[b,c]

It is known that the use of magnesium doped znic oxide (ZnMgO) nanoparticles results in a serious exciton quenching and unbalanced charge carriers inside the quantum dot light-emitting diodes (QLEDs), leading to an inferior device performance (particularly in blue QLEDs). Herein, we use water as a passivation agent to fix the interface between QDs and ZnMgO. On the one hand, the oxygen atoms in water could react with metal atoms to fill the oxygen vacancies on the surface of ZnMgO and remove the surface defects so that the excitons formed inside QDs are less quenched. On the other hand, it slightly decreases the electron transport from ZnMgO to QDs, resulting in much more balanced holes and electrons inside the QD emissive layers. Therefore, the blue QLEDs made by the water-passivated ZnMgO exihibit an improved external quantum efficiency (EQE) of 11.0% and luminance of over 20000 cd m^{-2} at 6V, which is significantly higher than those of blue QLEDs made by pristine ZnMgO. To further understand the improved performance among the blue QLEDs, the photoluminescence (PL) spectroscopy, transmission electron microscopy (TEM) and X-ray photoelectron spectroscopy (XPS) were used to characterize these water-passivated ZnMgO nanoparticles.

Introduction

Due to the interesting features such as high photoluminescence yields (PLQYs), tunable and saturated emission colours, and solution processibility, colloidal quantum dots (QDs) have a great potential to be one of the most efficient light-emitting materials used in lighting and displays, taking QDs based light-emitting diodes (QLEDs) as an example.[1–5] The typical and sandwich-like QLEDs consist of anodes and cathodes, electron/hole injection and transporting layers (EILs/HILs, ETLs/HTLs) and QD emissive layers (EMLs).[6,7] In general, hole transporting polymers such as poly (9,9-dioctylfluorene-co-N-(4-(sec-butyl)phenyl)diphenylamine) (TFB), poly(9-vinylcarbazole) (PVK) and poly(N,N'-bis(4-butylphenyl)-N,N'-bis(phenyl)benzidine (Poly-TPD) are commonly used as the HTLs.[8–10] It is found that the highest occupied molecular orbitals (HOMOs) of these polymers are around −5.5 eV, resulting in a significant valence band (VB) offset respect to the zinc sulfide (ZnS, VB = −6.9 eV) shells of QDs.[11,12] The hole injection and transportation from the HOMOs of hole transporting polymers to VBs of QDs are hampered.[13–16] Meanwhile, the ETLs consisting of zinc oxide (ZnO) nanoparticles (NPs) could deliver much more electrons inside the QDs due to their high conductivities and well-matched energy levels of their conduction bands (CBs).[17] Therefore, the holes and electrons inside the QD EMLs are unbalanced. On the other hand, a significant exciton quenching of QDs by the defects of ZnO NPs is generally observed.[18–20] It is noted that the performance of QLEDs will be restricted by the synergy of unbalanced charge carriers and serious exciton quenching.

To solve these problems, some strategies using interlayers to modify the QDs/ZnO interface and cations doped ZnO NPs are developed. For example, in 2014, Peng and coworkers inserted an insulating PMMA (poly(methyl methacrylate)) thin film between QDs and ZnO NPs to achieve efficiently red QLEDs with external quantum efficiencies (EQEs) of over 20%.[18] The use of insulating PMMA not only retards the electron transportation from ZnO NPs to QDs but also keeps the excitons formed inside the QDs from being quenched by the defects on the surfaces of ZnO NPs. Later, the literature reports focusing on improving the QDs/ZnO interfaces are emerging in a large number. Other organic polymers such as polyetherimide (PEI) and polyethylenimine ethoxylated (PEIE) could be used as the interlayers to improve the performance of QLEDs.[21,22] In general, these interlayers are ultrathin and hard to reproduce. Meanwhile, these insulating interlayers may afford the QLEDs with low luminance values and high applied voltages.[18,21,22] On the other hand, some cations with small atomic radii such as magnesium (Mg), aluminum (Al) and alkali metals (lithium (Li), sodium (Na) and potassium (K)) are doped into the ZnO NPs to significantly reduce the defects.[23–25] For example, Peng and coworkers continued their research on achieving highly efficient insulating-layer-free QLEDs by using Mg doped ZnO (ZnMgO) NPs in 2018. The use of ZnMgO could keep the excitons of QDs from being quenched. Meanwhile, tuning

a. *School of Applied Physics and Materials, Wuyi University, Jiangmen 529020, P. R. China.*
   E-mail: chenzhao2006@163.com; wdsongwyu@163.com
b. *Department of Applied Biology and Chemical Technology and Research Institute for Smart Energy, The Hong Kong Polytechnic University, Hung Hom, Hong Kong, P.R. China.*
c. *Hong Kong Polytechnic University Shenzhen Research Institute, Shenzhen 518057, P.R. China.*
   E-mail: wai-yeung.wong@polyu.edu.hk

the thickness of ZnMgO NPs achieves balance recombination of charge carrier inside the QD EMLs. Therefore, the red and green QLEDs exhibit an excellent performance, affording the peak EQEs of around 18% with long operation stabilities.[25] It is noted that most of the research works about the cations doped ZnO NPs focus on the applications in the red and green QLEDs and pay less attention to the blue QLEDs.[26] In general, due to the large energy gaps and high-energy excitons of blue QDs, the excitons inside the blue QD EMLs are much more vulnerable to the defects of ZnO NPs. It seems that the ZnMgO NPs may not be good enough to solve this problem.

Herein, trace water (H_2O) is added into the ZnMgO NPs to fill the oxygen vacancies on the surface of NPs, not only passivating the surface defects but also slowing down the electron injection and transportation into the blue QD EMLs. The blue QLEDs fabricated by using these H_2O-passivated ZnMgO (ZnMgO/H_2O) NPs as the ETL exhibit an improved performance with the peak EQE of 11.0% and luminance (L) of 21339 cd m^{-2} at 6 V, significantly superior to the blue QLEDs made by the pristine ZnMgO NPs (EQE$_{max}$ = 5.4%, L = 13805 cd m^{-2}). Meanwhile, the operational lifetime of the blue QLEDs based on the ZnMgO/H_2O ETL is longer than its reference QLEDs. The ZnMgO/H_2O NPs were also investigated by photoluminescence (PL) spectroscopy, transmission electron microscopy (TEM), X-ray photoelectron spectroscopy (XPS), X-ray diffraction (XRD), and hole/electron-only devices (HODs and EODs). From these results, it is found that the surface of ZnMgO/H_2O NPs possesses a much better crystal quality with less defects and oxygen vacancies so that the excitons inside the blue QDs are less quenched by the ZnMgO/H_2O NPs in comparison with the pristine ZnMgO NPs. Therefore, the ZnMgO/H_2O ETL affords its blue QLEDs with high efficiencies and long stabilities.

The blue QLEDs were fabricated by using the device architecture of ITO (indium tin oxide)/poly(3,4-ethylenedioxythiophene):poly(styrenesulfonate) (PEDOT:PSS, ~35 nm)/TFB (~30 nm)/blue QDs(~15 nm)/ETL (~50 nm)/Al (100 nm) (Figure 1a). Firstly, the ITO substrates were pre-cleaned in an ultrasonic cleaner with detergent and deionized water. After UV-O$_3$ treatment for 30 minutes, PEDOT:PSS (HIL, ~35 nm) was spin-coated on the ITO substrates and annealed at 150 °C for 15 min in air. Secondly, after transferring the ITO substrates into a nitrogen filled glove box, the HTL and EML films were fabricated in sequence by spin-coating the TFB polymer (8 mg mL^{-1} in chlorobenzene) and blue QDs (10 mg mL^{-1} in octane) on the surface of PEDOT:PSS and annealing at 120 and 90 °C for 10 and 5 minutes, respectively. Thirdly, ZnMgO with or without trace water (20 mg mL^{-1} in ethanol) was spin-coated and annealed at 60 °C (10 minutes) to form the ETL (~ 50 nm). To prepare the solutions of ZnMgO/H_2O NPs, 20 μL deionized water were added into 10 mL ethanol. To investigate the influence of water dosage on the performance of blue QLEDs, the synthetic ZnMgO NPs were diluted to 20 mg/mL by using the ethanol/H_2O solutions with different volume values of water (0, 10, 20 and 40 μL) (See Electronic Supporting Information (ESI), Preparation of ZnMgO nanoparticles). These ZnMgO/H_2O NPs were placed into a nitrogen filled glove box overnight before use. Some white precipitates are easily observed in these ZnMgO NP solutions

with much more water dosages (> 40 μL), which afford the ZnMgO ETLs with a poor film quality. Meanwhile, a large water dosage results in a significant increase of H_2O in the glove box. Therefore, to ensure the trace H_2O content in the glove box lower than the threshold value detected by the probe, the use of ethanol/H_2O solution should be finely controlled. Lastly, Al (anode, 100 nm) was thermally deposited under a pressure of 2×10^{-6} torr. The active area of these blue QLEDs was 2 mm ☒ 2 mm and the devices were encapsulated before measurement. The current−voltage (I−V) curves were measured by a dual-channel Keithley 2400 source meter. By using an integrating sphere and multi-channel analyzer PMA−12, the EL spectra, luminance values and EQEs were collected by an external quantum efficiency measurement system (C9920−12, Hamamatsu Photonics, Japan).[27]
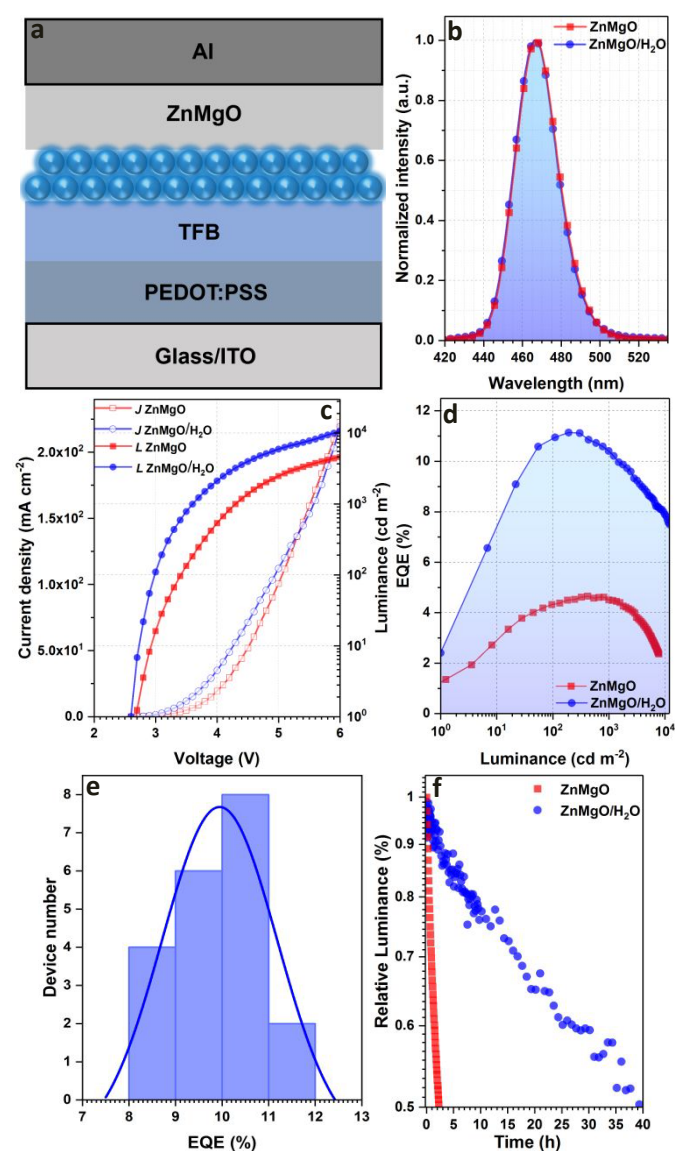

Figure 1. EL performance of the best blue QLEDs based on ZnMgO and ZnMgO/H_2O ETLs: a) the device structure; b) EL spectra; c) current density-voltage-luminance curves; d) EQE *vs* luminance

curves; e) EQE reproducibility and f) operational lifetimes (L_0 = 700 cd m^{-2}).

As shown in Figure 1b and S1a, the electroluminescence (EL) spectra of these devices made by different ZnMgO NPs are consistent, corresponding to the fact there is no influence of the trace water in the ZnMgO NPs on the EL spectra of blue QLEDs. As shown in Figure S1, the best blue QLED is fabricated by using the ZnMgO/H$_2$O NPs with 20 μL water dosage. Possibly, an inefficient surface passivation occurs when less water dosage is used. Meanwhile, the large water dosage may result in the poor film quality since water is a poor solvent to precipitate the ZnMgO NPs. Here, we only discuss the best ZnMgO/H$_2$O system in this manuscript. The L value of 21339 cd m^{-2} at 6 V is found for the blue QLED made by ZnMgO/H$_2$O ETL in the current density–voltage–L (J–V–L) curves (Figure 1c), significantly higher than that of the blue QLED (L = 13805 cd m^{-2}) based on the pristine ZnMgO NPs. The high luminance of the device corresponds to a much more efficient radiation from the excitons formed by the recombination of charge carriers.[28] It is noted that the peak EQE of the blue QLED based on the ZnMgO/H$_2$O ETL is 11.0%, at least two times higher than that of device made by the pristine ZnMgO NPs (EQE$_{max}$ = 5.4%) (Figure 1d). The ZnMgO/H$_2$O based blue QLEDs exhibit a good EQE reproducibility and most values are higher than 10% (Figure 1e). Meanwhile, the device fabricated by the ZnMgO/H$_2$O ETL also possesses a longer device operation lifetime. When the luminance is decreased to the half of its initial value (700 cd m^{-2}), the operational lifetime (T_{50}) of the blue QLED by using the ZnMgO/H$_2$O ETL is around 40 hours, which is significantly longer than it reference device (T_{50} = 2.3 hours) (Figure 1f). In addition, these two ZnMgO ETL afford their blue QLEDs with a low turn-on voltage (V_{on}) of 2.6 V (Figure 1c). From these results, we believe that the ZnMgO/H$_2$O NPs could be one of excellent ETLs for the blue QLED application.

Firstly, due to the well-matched size between the oxygen vacancies and oxygen atoms, the added water with a small molecule volume can precisely fill these vacancies of ZnMgO NPs. To confirm this hypothesis, X-ray photoelectron spectroscopy (XPS) was used to reveal the influence of water on the vacancies of ZnMgO NPs. As shown in Figure 2, the added water mainly influences the O 1s peak and no remarkable change is found in the Zn 2p and Mg 1s spectra. The peaks located at 532.0, 531.2 and 530.0 eV are assigned to the hydroxyl bond (O$_H$), oxygen vacancy (O$_V$) and metal–oxygen bond (O$_M$), respectively (Figure 2a and 2b).[29,30] The total integral area of the O 1s spectrum was normalized and considered as 100%. It is noted that the intensity of O$_V$ in the ZnMgO/H$_2$O film is decreased with a ratio of 25.5%, which is lower than that of the pristine ZnMgO NPs (32.9%) (Figure 2b). A ratio difference of 7.4% between the proportion values of pristine ZnMgO and ZnMgO/H$_2$O is observed. The O$_V$ contains two types, the inside and surface vacancies. By considering that the total volume of the H$_2$O molecule is slightly bigger than the size of oxygen vacancy, the inward permeation of H$_2$O to the deep inside ZnMgO NPs is limited. We believe that the added water only fills the vacancies on the surface of ZnMgO NPs and has no influence on these vacancies inside the NPs (Figure 3). After

adding water, the ratio of O$_H$ is increased from 37.3% (ZnMgO NPs) to 53.1% (ZnMgO/H$_2$O NPs) due to the two O–H chemical bonds in H$_2$O. The ascending proportion of O$_H$ (15.8%) is almost twice as much as the descending proportion of O$_V$ (7.4%) (Figure 2a and 2b). Therefore, the added H$_2$O may not react with the metal (M) to form the M–O–H chemical bonds. It seems that the added trace water has less influence on the M–O chemical bonds because there are no newly formed M–O chemical bonds. It is different from other previous reports that the
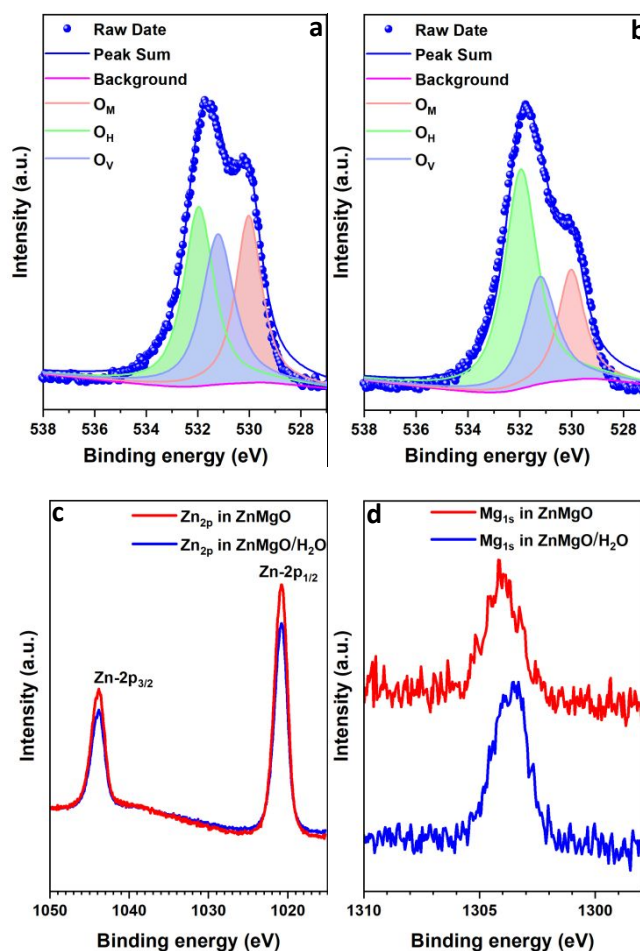

Figure 2. a) and b) The O 1s spectra of ZnMgO and ZnMgO/H$_2$O NPs, respectively; c) the Zn 2p and d) Mg 1s spectra of ZnMgO and ZnMgO/H$_2$O NPs.

Zn–O–H chemical bonds is formed by the reaction of the trace H$_2$O and Zn ions in the presence of oxygen radicals.[31] It is found that the intensity of O$_M$ in the O 1s spectra of the ZnMgO/H$_2$O NPs is decreased by 8.4% (Figure 2a and 2b). This value corresponds to the increased O$_H$ proportion when the water is added into the ZnMgO NPs. It is noted that two O–H chemical bonds are found in one H$_2$O molecule. The doubly increased O$_H$ will be bonded to own an over high percentage so that the O$_M$ intensity is shrunk. Therefore, we believe that the added H$_2$O may not react with the metal to form the M–O chemical bonds and therefore the O$_M$ percentage should be unchanged. Based on these, there is one feasible adsorption

approach through the physical adsorption based on an electrostatic interaction between the electron-rich oxygen atoms and positive Zn^{2+} ions, accelerating the added water to fill the surface oxygen vacancies (Figure 3b). From the XPS results, the oxygen vacancies on the surface of ZnMgO NPs could be passivated by water, making the QD surface far from the surface defects of ZnMgO NPs.
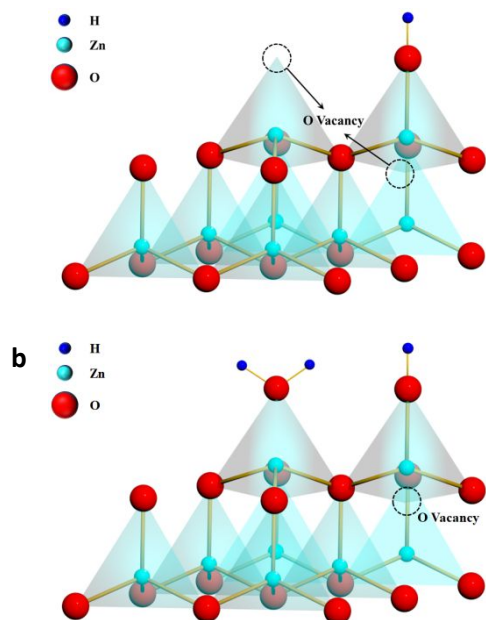

Figure 3. The schematic diagrams of a) oxygen vacancies in pristine ZnMgO NPs and b) the H_2O on the surface of ZnMgO/H_2O NPs.

Secondly, the spectra of UV-visible absorption and photoluminescence (PL) and the PL decay curves for these ZnMgO NPs were firstly studied. From the absorption spectra in Figure 4a, there is almost no difference observed from these curves, which reveals that the addition of water has no or less influence on the absorption properties of these ZnMgO NPs. Meanwhile, a decreased emission intensity at around 540 nm is observed for the ZnMgO/H_2O film (Figure 4b). As we know, this emission peak is due to the defects of ZnMgO NPs and its intensity is positively related to the defect scale.[18,32] Therefore, the weak emission at 540 nm in the PL spectrum of ZnMgO/H_2O film corresponds to less defects in ZnMgO/H_2O NPs, which is also confirmed the PL spectra and PL decay curves of the blue QDs (Figure 4c and 4e). The defects of ZnMgO NPs will seriously quench the excitons of QDs at the interface of QD/ZnMgO films, resulting in a significant decrease of QD emission (Figure 4c, green line). Fortunately, there is only slight intensity decrease after adding trace H_2O into the ZnMgO NPs (Figure 4c, red line). In addition, the PL decay curves for the BQD and ZnMgO/H_2O/BQD films are monoexponential with the lifetime (τ) values of 5.0 and 4.2 ns, respectively (Figure 4d). A double-exponential process is observed in the PL decay curve of the ZnMgO/BQD film. The τ_1 and τ_2 are 1.6 and 3.3 ns with the amplitude values (A_1 and A_2) of 59.0% and 41.0%, respectively, corresponding to an average lifetime of 2.6 ns. The double-exponential decay curve of ZnMgO/BQD film may be due to two PL decay processes, one of which is resulted from the effect of

the surface defects in the ZnMgO film.[33] It is noted that the τ value of the ZnMgO/H_2O/BQD film is slightly shorter than that of the BQD film but significantly higher than that of ZnMgO/BQD. Therefore, less excitons inside the BQD film are quenched by the ZnMgO/H_2O film in comparison with the ZnMgO film. As we know, the surface defects of ZnMgO NPs will trap the holes inside the QDs and therefore quench the excitons of QDs (Figure 4e).[31] Once the defects are passivated by the added water, the hole trap will be restrained (Figure 4f), resulting in the less exciton quenching and therefore the longer τ values. According to the XPS results, we believe that the less exciton quenching inside the blue EMLs is due to the fact that the added water protects these QDs from being directly exposed to the defects of ZnMgO when the ZnMgO/H_2O NPs is used.
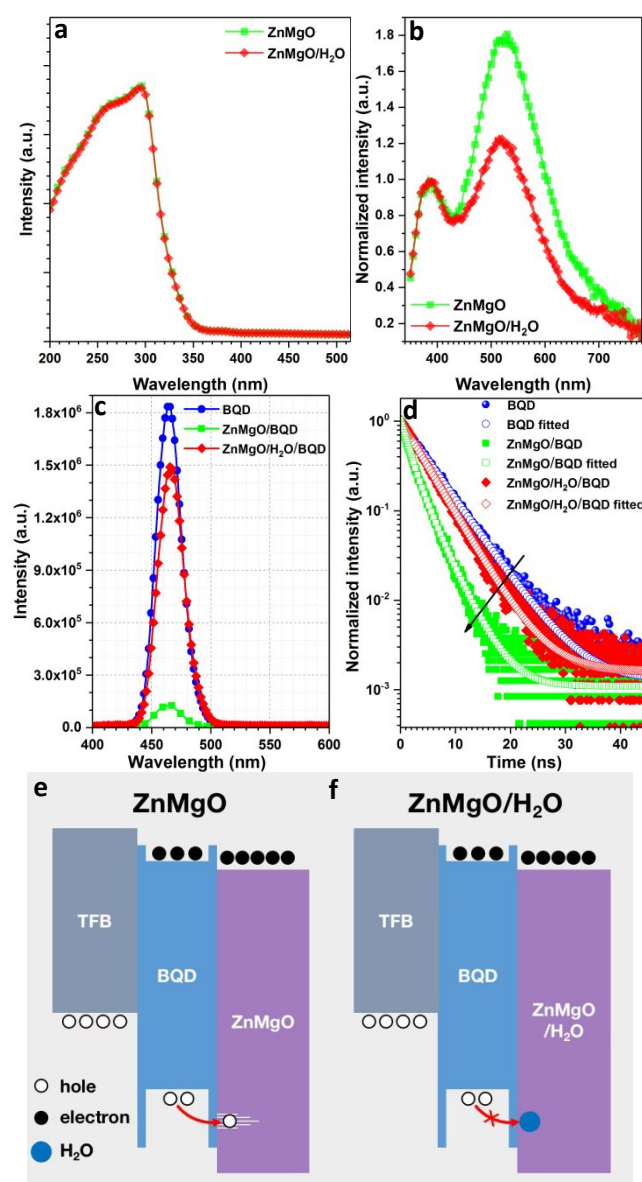

Figure 4. a) and b) UV-visible absorption and PL spectra of ZnMgO film; c) and d) steady and transient PL spectra of ZnMgO/QD films; the schematic diagrams of e) exciton quenching and f) restricted exciton quenching at the interface of QD/ZnMgO.

Thirdly, according to the previous reports, the passivated ZnMgO may affect the electron injection and transport from the ZnMgO ETL to the QD EMLs. To investigate the influence of added water on the injection and transport of electrons, the capacitance–voltage (C–V) curves of blue QLEDs and J–V curves of the hole-only devices (HODs) were characterized. As shown in Figure 5a, the capacitance (C_p) is gradually increased when the applied voltage is higher than the transition voltage (V_t), corresponding to the injection and accumulation of charge carriers in the QD EMLs.[34] By considering that a much more significant energy barrier for hole transport from the HOMO of TFB to the VB of QD EML than the electron transport from the ZnMgO ETL to the QD EML, we believe the electrons are first injected and accumulated in these blue QLEDs. It is noted that the two blue QLEDs possess a similar V_t of around 2.0 V, which reveals that the energy barriers for the electron injection from the pristine ZnMgO and ZnMgO/H_2O ETLs to QDs are almost the same. It is confirmed by the unchanged CB and VB energy levels of these two ZnMgO NPs (Figure 4a and Figure S3). Meanwhile, characteristic voltage (V_c) values are observed when the capacitance values reach their peaks (C_p). The hole injection occurs and these injected holes will recombine with the accumulated electrons inside the QD EMLs, resulting in the decreased C_p values after the recombination of charge carriers. As we know, the blocking of electron injection results in a decreased electron density inside the EMLs. Once the holes are injected, these electrons will immediately be consumed through the recombination of charge carriers, affording the devices with smaller V_c and C_p values.[34] Therefore, the decreased V_c and C_p values in the device made by the ZnMgO/H_2O ETL demonstrate that the added water can decrease the electron injection and transport from the ZnMgO/H_2O ETL to QD EML,
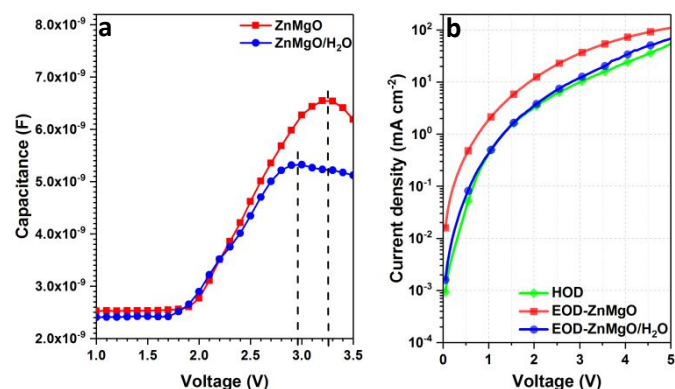

Figure 5. a) The capacitance–voltage curves of the blue QLEDs made by ZnMgO and ZnMgO/H_2O ETLs; b) the current density–voltage curves of single charge carrier-only devices.

which is also confirmed by the electron-only devices (EODs). It is found that the current density of the EOD with the device structure of ITO/ZnMgO/H_2O/BQD/H_2O/ZnMgO/Al is significantly lower than that of EOD based on the pristine ZnMgO NPs, corresponding to a relatively weak electron conductivity of the ZnMgO/H_2O ETL. Meanwhile, the current density of the EOD based on the ZnMgO/H_2O ETL can well match with that of the hole-only device (HOD) (device structure: ITO/PEDOT:PSS/TFB/BQD/MoO$_3$/Al) (Figure 5b). By

combining with the results found in the capacitance–voltage curves, we believe that the electrons and holes inside the EMLs of the blue QLEDs based on the ZnMgO/H_2O ETL are balanced so that a balanced recombination between these charge carriers occurs and therefore an efficient radiation occurs.[28,34]

Other characteristics containing the nanocrystal morphology, X-ray diffraction (XRD) and ultraviolet photoelectron spectroscopy (UPS) were also used to investigate the difference between the ZnMgO/H_2O and pristine ZnMgO NPs. As shown Figure 6, the added water may not change the size of NPs, retaining the size values of around 5 nm for both ZnMgO and ZnMgO/H_2O NPs. With a high magnification, there is almost no morphology difference on the surface of ZnMgO NPs. It may reflect that the added water has less influence on the ZnMgO crystal quality, which agrees with the result that no crystallinity change is observed from the XRD spectra (Figure S4). Besides, the UPS results reveal that the VBs of these NPs are around –7.0 eV, corresponding to less influence of the added water on the VB and CB energy levels of these ZnMgO NPs.
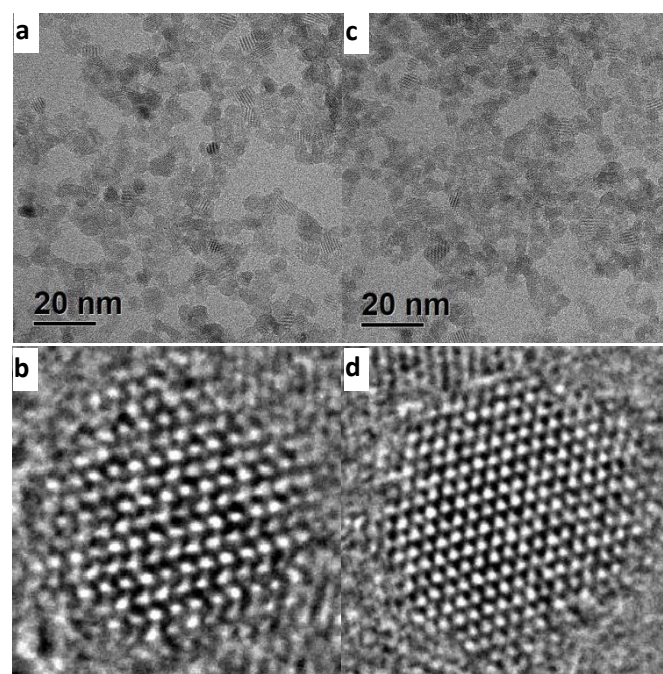

Figure 6. Transmission electron microscope (TEM) images of a),b) ZnMgO and c),d) ZnMgO/H_2O NPs.

Conclusions

In conclusion, a simple and efficient approach to passivate the defects of ZnMgO NPs is developed by adding trace water into the ZnMgO solution. The blue QLED based on the water passivated ZnMgO/H_2O ETL exhibits a better performance with the peak EQE of 11.0%, luminance value of 21339 cd m^{-2} at 6 V and operation lifetime of 40 hours, which are superior to its reference device (EQE$_{max}$ = 5.4%, L = 13805 cd m^{-2} and T_{50} = 2.3 hours) based on the ZnMgO ETL. To investigate the reason why the ZnMgO/H_2O NPs could improve the performance of the blue QLEDs, the characteristics comprising XPS, steady and transient

PL spectra, capacitance and single charge carrier-only devices were conducted. From the results of XPS, we believe that the added water could make the QDs far from the surface defects of ZnMgO NPs through the electrostatic interaction based physical adsorption formed between the oxygen atoms and zinc ions, resulting in the decreased oxygen vacancies on the surface of ZnMgO NPs. It passivates the ZnMgO surface and protects the excitons inside the QD EML from being quenched, which is confirmed by the results measured from the PL spectra. Less exciton quenching inside the blue EML affords the blue QLED made by the ZnMgO/H_2O ETL with a strong radiation from the blue QDs. Meanwhile, both the capacitance–voltage curves of the blue QLEDs and current density–voltage curves of single charge carrier-only devices reveal the fact that the added water slows down the electron injection and transport from the ZnMgO ETL to the QD EML and results in a much more balanced charge carriers inside the QD EML, corresponding to an

and balanced recombination of these charge carriers.

the synergy between the balanced charge carriers and less exciton quenching inside the blue EML result in the excellent performance of the blue QLED fabricated by the ZnMgO/H_2O ETL. From these results, it demonstrates that the surface defects of ZnMgO are easily passivated by the water and the water-passivated ZnMgO NPs could be an efficient ETL useful for the blue QLEDs.

Acknowledgements

Notes and references

1   H. Moon, C. Lee, W. Lee, J. Kim, H. Chae, *Adv. Mater.*, 2019, **31**, 1804294.
2   Z. Yang, M. Gao, W. Wu, X. Yang, X. W. Sun, J. Zhang, H.-C. Wang, R.-S. Liu, C.-Y. Han, H. Yang, W. Li, *Mater. Today*, 2019, **24**, 69.
3   X. Dai, Y. Deng, X. Peng, Y. Jin, *Adv. Mater.*, 2017, **29**, 1607022.
4   H. Cho, J.-A. Pan, H. Wu, X. Lan, I. Coropceanu, Y. Wang, W. Cho, E. A. Hill, J. S. Anderson, D. V. Talapin, *Adv. Mater.*, 2020, **32**, 2003805.
5   E. Nannen, J. Frohleiks, S. Gellner, *Adv. Funct. Mater.*, 2020, **30**, 1907349.
6   H. Jia, F. Wang, Z. Tan, *Nanoscale*, 2020, **12**, 13186.
7   H. Qi, S. Wang, X. Jiang, Y. Fang, A. Wang, H. Shen, Z. Du, *J. Mater. Chem. C.*, 2020, **8**, 10160.
8   M. Redecker, D. D. C. Bradley, M. Inbasekaran, W. W. Wu, E. P. Woo, *Adv. Mater.*, 1999, **11**, 241.
9   M. D. Ho, D. Kim, N. Kim, S. M. Cho, H. Chae, *ACS Appl. Mater. Interfaces*, 2013, **5**, 12369.
10 X. Zhao, Z.-K. Tan, *Nat. Photonics*, 2020, **14**, 215.
11 J. Song, O. Wang, H. Shen, Q. Lin, Z. Li, L. Wang, X. Zhang, L. S. Li, *Adv. Funct. Mater.*, 2019, **29**, 1808377.
12 H. Shen, W. Cao, N. T. Shewmon, C. Yang, L. S. Li, J. Xue, *Nano Lett.*, 2015, **15**, 1211.
13 H. Jia, F. Wang, Z. Tan, *Nanoscale*, 2020, **12**, 13186.
14 H. Qi, S. Wang, X. Jiang, Y. Fang, A. Wang, H. Shen, Z. Du, *J. Mater. Chem. C*, 2020, **8**, 10160.
15 P. Reiss, M. Protière, L. Li, *Small*, 2009, **5**, 154.
16 L. Xie, X. Xiong, Q. Chang, X. Chen, C. Wei, X. Li, M. Zhang, W. Su, Z. Cui, *Small*, 2019, **15**, 1900111.
17 E. Moyen, J. H. Kim, J. Kim, J. Jing, *ACS Appl. Nano Mater.*, 2020, **3**, 5203.
18 X. Dai, Z. Zhang, Y. Jin, Y. Niu, H. Cao, X. Liang, L. Chen, J. Wang, X. Peng, *Nature*, 2014, **515**, 96.
19 M. C. Löbl, C. Spinnler, A. Javadi, L. Zhai, G. N. Nguyen, J. Ritzmann, L. Midolo, P. Lodahl, A. D. Wieck, A. Ludwig, R. J. Warburton, *Nat. Nanotechnol.*, 2020, **15**, 558.
20 J. P. Philbin, E. Rabani, *J. Phys. Chem. Lett.*, 2020, **11**, 5132.
21 K. Ding, H. Chen, L. Fan, B. Wang, Z. Huang, S. Zhuang, B. Hu, L. Wang, *ACS Appl. Mater. Interfaces*, 2017, **9**, 20231.
22 Y.-L. Shi, F. Liang, Y. Hu, M.-P. Zhuo, X.-D. Wang, L.-S. Liao, *Nanoscale*, 2017, **9**, 14792.
23 J.-H. Kim, C.-Y. Han, K.-H. Lee, K.-S. An, W. Song, J. Kim, M. S. Oh, Y. R. Do, H. Yang, *Chem. Mater.*, 2015, **27**, 197.
24 R. Azmi, S. Hwang, W. Yin, T.-W. Kim, T. K. Ahn, S.-Y. Jang, *ACS Energy Lett.*, 2018, **3**, 1241.
25 Z. Zhang, Y. Ye, C. Pu, Y. Deng, X. Dai, X. Chen, D. Chen, X. Zheng, Y. Gao, W. Fang, X. Peng, Y. Jin, *Adv. Mater.,* 2018, **30**, 1801387.
26 F. Wang, W. Sun, P. Liu, Z. Wang, J. Zhang, J. Wei, Y. Li, T. Hayat, A. Alsaedi, Z. Tan, *J. Phys. Chem. Lett.*, 2019, **10**, 960.
27 H.-W. Mo, Y. Tsuchiya, Y. Geng, T. Sagawa, C. Kikuchi, H. Nakanotani, F. Ito, C. Adachi, *Adv. Funct. Mater.*, 2016, **26**, 6703.
28 H. Shen, Q. Gao, Y. Zhang, Y. Lin, Q. Lin, Z. Li, L. Chen, Z. Zeng, X. Li, Y. Jia, S. Wang, Z. Du, L. S. Li, Z. Zhang, *Nat. Photonics*, 2019, **13**, 192.
29 J. E. Yeom, D. H. Shin, R. Lampande, Y. H. Jung, N. N. Mude, J. H. Park, J. H. Kwon, *ACS Energy Lett.*, 2020, **5**, 3868.
30 Y. Lee, H.-M. Kim, J. Kim, J. Jang, *J. Mater. Chem. C*, 2019, **7**, 10082.
31 M. Chrzanowski, G. Zatryb, P. Sitarek, A. Podhorodecki, *ACS Appl. Mater. Interfaces*, 2021, **13**, 20305.

32 Y. Sun, W. Wang, H. Zhang, Q. Su, J. Wei, P. Liu, S. Chen, S. Zhang, *ACS Appl. Mater. Interfaces*, 2018, **10**, 18902.

33 S. A. Jenekhe, J. A. Osaheni, *Science*, 1994, **265**, 765.

34 H. Zhang, S. Chen, *J. Mater. Chem. C*, 2019, **7**, 2291.